SUPPLEMENTARY MATERIAL

In-situ integration of bimetallic NiFe Prussian blue analogs on carbon cloth for oxygen evolution reaction

Zhiyong Wang,[#a,d] Shusheng Wan, [#b] Yuanmao Chen,[a,d] Juntao Ren,*[e] Lin Liu,[c] Panpan Yuan,[c] Qiong Luo,[c] Peng Deng,[c] Zheng Liang, [a,d] Xinyang Yue,*[a,d] Junxiong Wang,*[a,d]

[a]Frontiers Science Center for Transformative Molecules, School of Chemistry and Chemical Engineering, Shanghai Jiao Tong University, Shanghai 200240, China.

[b]School of Mechanical Engineering, Shanghai Jiao Tong University, Shanghai 200240, China.

[c]School of Materials Science and Engineering, Jiangxi University of Science and Technology, Ganzhou 341000, China.

[d]Zhangjiang Institute for Advanced Study, Shanghai Jiao Tong University, Shanghai, 200240, China.

[e]Department of Catalytic Materials, Henan Newmight Company, Xuchang 461700, China.

[#] These authors contributed equally to this work.

* Corresponding author: hfhgchrjt@163.com (J. Ren);
xinyangyue@sjtu.edu.cn (X. Yue);
wjx1992@sjtu.edu.cn (J. Wang);

Experimental Section

Chemicals and reagents

Potassium hexacyanoferrate (III) ($K_3[Fe(CN)_6]$, 99%) and polyvineypirrolydone (PVP, K30, MW ~ 40000) were purchased from Shanghai Macklin Biochemical Co., Ltd. (Shanghai, China). Nickel chloride ($NiCl_2·6H_2O$), sodium citrate dihydrate ($C_6H_5Na_3O_7$) and concentrated hydrochloric acid (HCl, 12 M) was obtained from Shanghai Aladdin Industrial Inc. (Shanghai, China). The carbon cloth (CC) (WOS1009, 20 cm × 20 cm) was purchased from CeTech CO., Ltd., China. Nickel foam (NF) (30 $mg·cm^{-2}$) was purchased from Changsha Lyrun Material Co., Ltd. (Changsha, China). The NF (1 cm × 1 cm) was firstly cleaned in 10 mL of isobutanol and 10 mL of deionized water in turn under the sonication for 10 min. Afterwards, the NF was soaked in 0.5 M H_2SO_4 solution for 30 min.

Fabrication of PB@CC

Firstly, a large sheet of CC (5 cm × 5 cm) was soaked in concentrated H_2SO_4 and HNO_3 (volume ratio = 3: 1) solution for 12 h. Then, a small piece (1 cm × 2 cm) was cut from the above CC and carefully washed with DI water and absolute ethanol in an ultrasound bath for 10 min, respectively. Secondly, the as-prepared CC and 2 mmol (0.66 g) $K_3[Fe(CN)_6]$ were added to 40 mL 0.1 M HCl solution in a 250 mL jar (Fig. S1c). After stirring for 5 min, 3 g PVP (K30) was added under magnetic stirring. the solution turned clear and became light yellow during stirring for 10 min. The jar was then transferred to an electric oven and sealed at 80 °C for 12 h. The ultramarine solution was then subjected to centrifugation with 5000 r/min, and the collected particles were washed several times with DI water and absolute ethanol. Finally, the PB standing on CC (PB@CC) was directly obtained after vacuum oven drying at 100 °C for 2 h. The mass loading of PB in the PB@CC is about 3 $mg\ mm^{-2}$.

Fabrication of NFPB@CC

Firstly, 0.6 mmol $NiCl_2·6H_2O$ and 1.0 mmol $C_6H_5Na_3O_7$ were dissolved in 20 mL deionized water under stirring for 10 min to obtain a homogeneous solution A. Meanwhile, 0.6 mmol of $K_3[Fe(CN)_6]$ was also dissolved in 20 mL deionized water with stirring for 5 min to obtain solution B. Subsequently, a small piece of the as-prepared

CC (1 cm × 2 cm) was put into the solution B under ultrasonication for 5 min. Then the solution A was added to solution B under continuously magnetic stirring for 10 min. The mixed solution became green after stirring and was transferred to a 250 mL jar (Fig. S1c). Finally, the jar was placed into an electric oven and sealed at 80 °C for 12 h. The yellow solution was then subjected to centrifugation with 5000 r/min, and the collected particles and NFPB standing on CC (NFPB@CC) were washed several times with DI water and absolute ethanol. The mass loading of NFPB in the NFPB@CC is about 2 mg mm^{-2}. The other two PBAs with varying Fe/Ni ratios were synthesized by adjusting the proportions of ingredient, which were labeled as NFPB-51, NFPB-31 and NFPB-11, respectively. And the detailed data are presented in Table S1.

Table S1

The NFPB samples prepared with different Ni/Fe ratios

Samples	Ni/Fe	$NiCl_2 \cdot 6H_2O$ (mmol)	$C_6H_5Na_3O_7$ (mmol)	$K_3[Fe(CN)_6]$ (mmol)
NFPB-51	5:1	1.0	1.7	0.2
NFPB-31	3:1	0.9	1.5	0.3
NFPB-11	1:1	0.6	1	0.6

Note: the solution volumes were 40 mL

Materials characterizations

The morphology of the fabricated materials was investigated by field-emission scanning electric microscopy (SEM, Supra 55 ZEISS; Sirion 200) with an acceleration voltage of 20 kV. The crystalline phase of the PB and NFPB was examined by powder X-ray diffraction (XRD, D8 DaVinci instrument). The microstructure and size of NFPB were characterized by field-emission transmission electron microscopy (TEM, TALOS F200X G2). Raman was used to investigate the samples (Renishaw inVia Qontor with 532 nm excitation wavelength laser). N_2 adsorption experiments using quantachrome measuring instruments (QuadraSorb Station 2) were carried out to investigate the porosity and pore size distribution of the sample. The specific surface area can be calculated using the multi-point Brunauer-Emmett-Teller (BET) equation. The mesopore size distribution was determined by the Barrett-Joyner-Halenda (BJH) method using the adsorption branch of the isotherm. The surface elements composition of the PB@CC and NFPB@CC was analyzed by an X-ray photoelectron

spectrometer (XPS, AXIS UltraDLD) with a monochromatic Al Kα X-ray source.

Electrochemical measurements

All electrochemical measurements were performed on the Chenhua electrochemical workstation (CHI 760E, Shanghai, China) using a standard three-electrode configuration in 1 M KOH solution (pH 14) at room temperature. The prepared samples, a Pt electrode, and a Hg/HgO electrode were used as the working, counter, and reference electrodes, respectively. The potentials presented were all relative to the reversible hydrogen electrode (*vs.* RHE), referring to the equation:

$$E\ (RHE) = E\ (Hg/HgO) + 0.924 + 0.059 \times pH$$

The linear sweep voltammogram (LSV) was tested from 0.135 V to 0.9 V at a scan rate of 10 mV s^{-1} with iR compensations. The Tafel slope can be derived from LSV results by the formula ($\eta = b \log |j| + a$). Electrochemical impedance spectroscopy (EIS) testing of the different samples was probed over the frequency from 1 Hz to 100 kHz at an electrolysis potential of 0.924 V vs. RHE with an AC amplitude of 5 mV. The electrochemical double-layer capacitance (C_{dl}) was examined from the cyclic voltammetry (CV) with various scan rates (20, 40, 60, 80, 100, 120 mV s^{-1}), which were recorded in a non-faradaic potential range (−0.1 ~ 0.1 V *vs.* Hg/HgO). The electrochemical active surface area (ECSA) was evaluated by C_{dl} values. The long-term stability was revealed by the chronopotentiometric tests at 10 mA cm^{-2}.

SI Figures and Movie

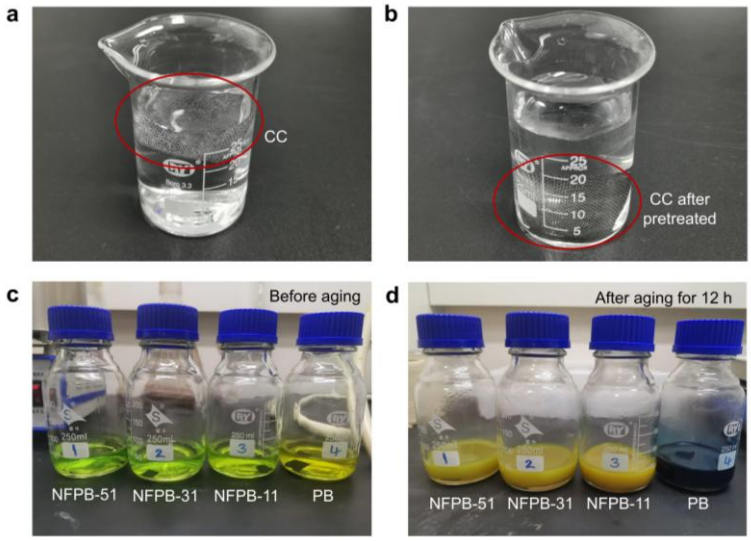

Fig. S1 Photographs of (a) CC and (b) the pretreated CC in the DI water. Photographs of synthetic solutions for PB and NFPB with different Ni/Fe ratios (c) before aging and (d) after aging for 12 h at 80 °C.

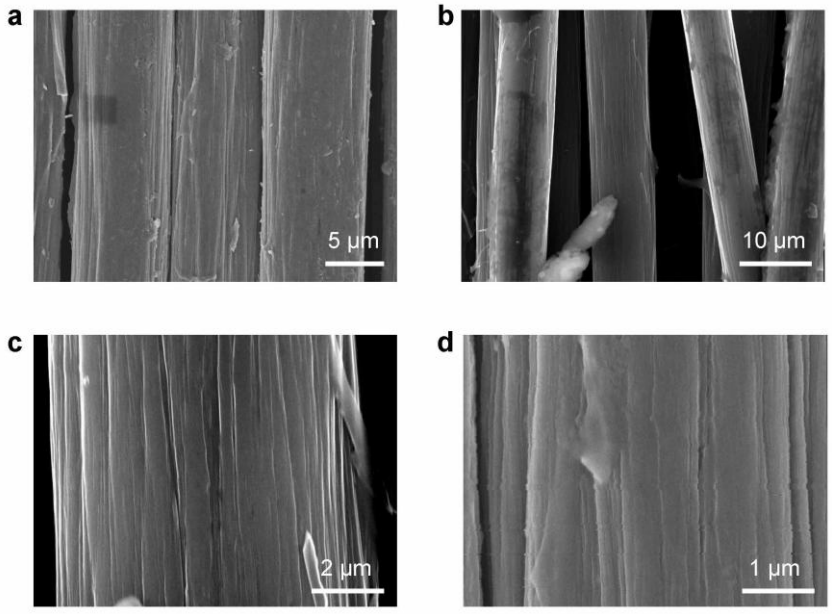

Fig. S2 (a~d) SEM images of the CC with different magnifications.

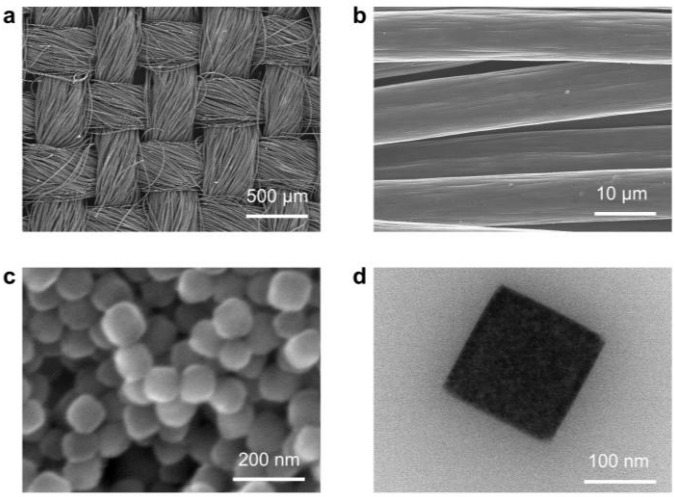

Fig. S3 (a, b) SEM images of the pretreated CC. (c) SEM image of PB particles. (d) TEM image of NFPB particle.

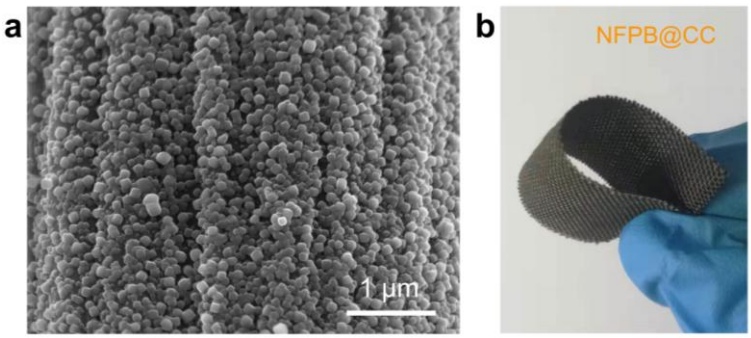

Fig. S4 (a) The SEM image of NFPB@CC. (b) The photograph of a flexible NFPB@CC.

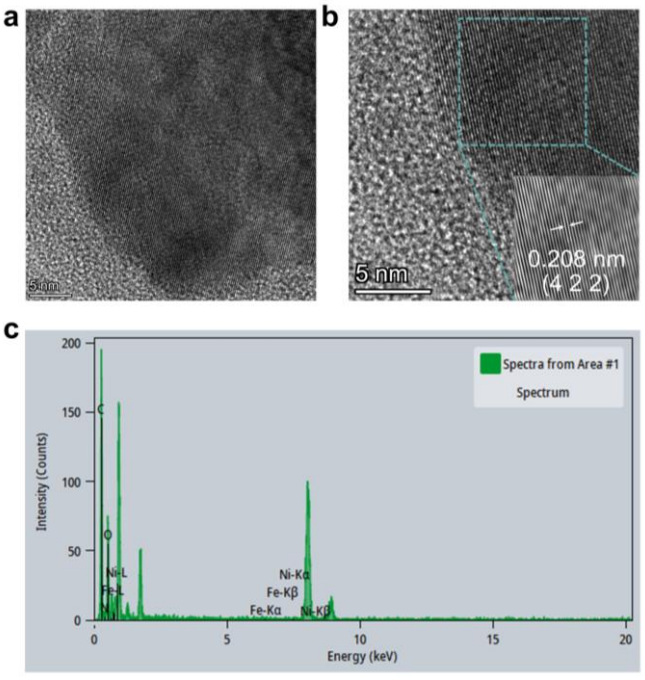

Fig. S5 (a, b) The HR-TEM images and (c) the corresponding energy dispersive X-ray

spectroscopy (EDS) of NFPB.

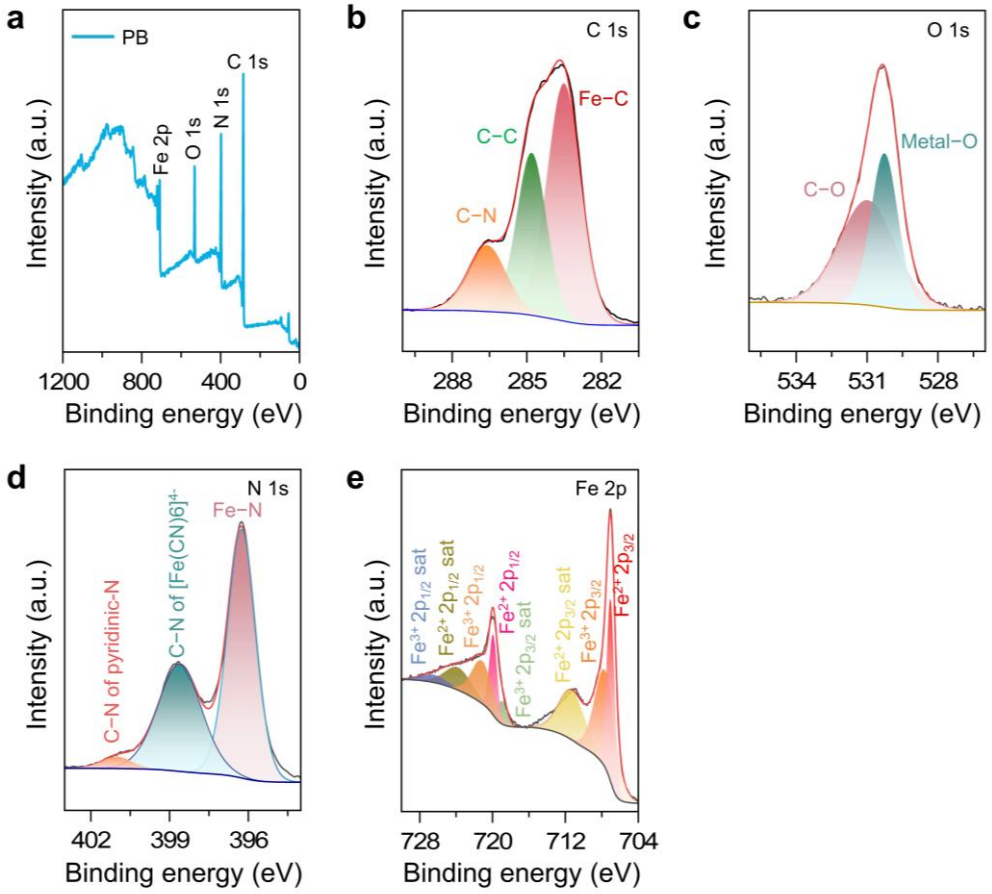

Fig. S6 (a) The XPS full spectrum of PB@CC. The XPS spectra of (b) C 1s, (c) O 1s, (d) N 1s, and (e) Fe 2p for PB@CC.

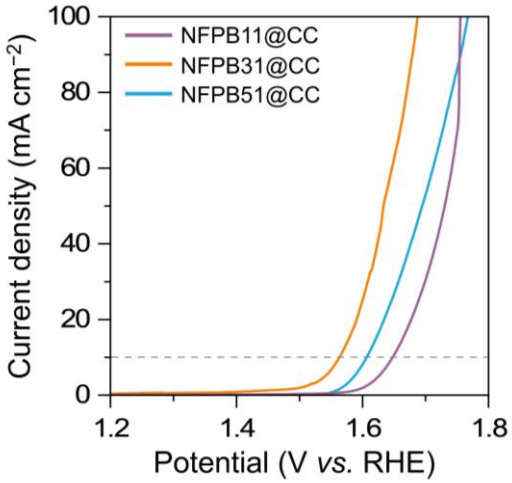

Fig. S7 The LSV curves of NFPB@CC with different Ni/Fe ratios.

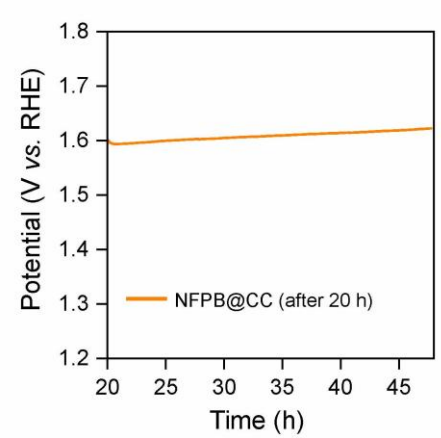

Fig. S8 The CP profile of NFPB@CC at 10 mA cm^{-2} after the first 20 h CP test.

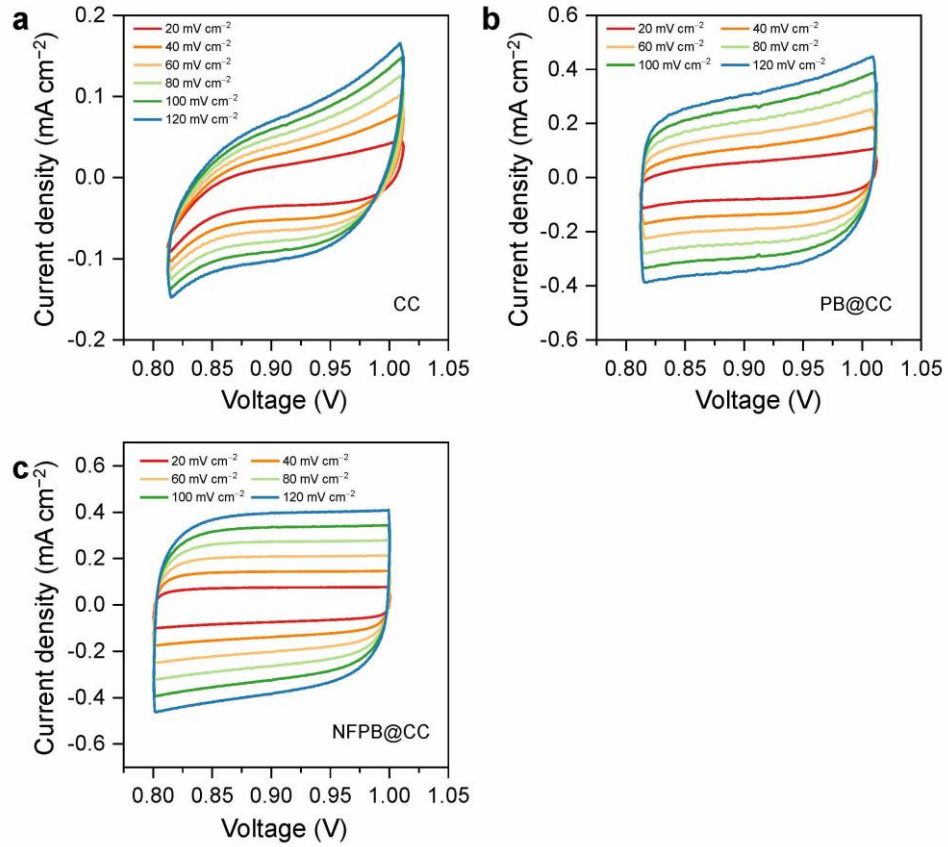

Fig. S9 CV curves of (a) CC, (b) PB@CC, and (c) NFPB@CC at different scan rates.

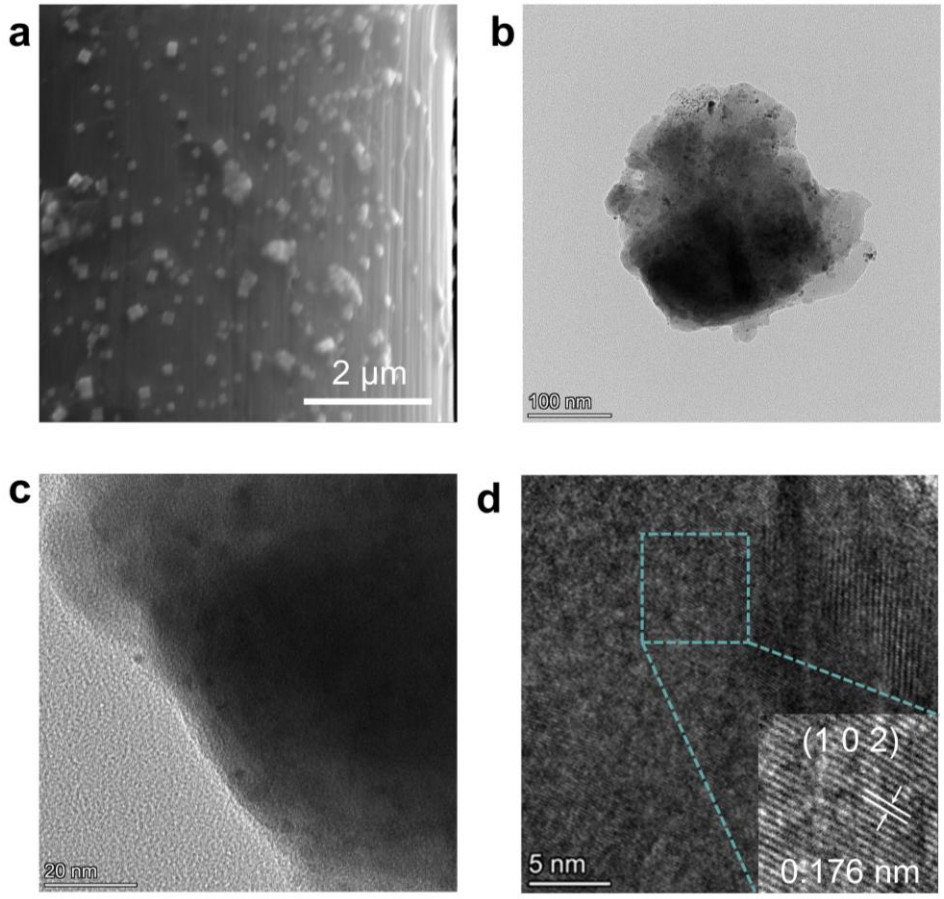

Fig. S10 (a) The SEM image of NFPB@CC after the CP test of 20 h. The corresponding (b, c) low-resolution TEM images and (d) HR-TEM image of NFPB.

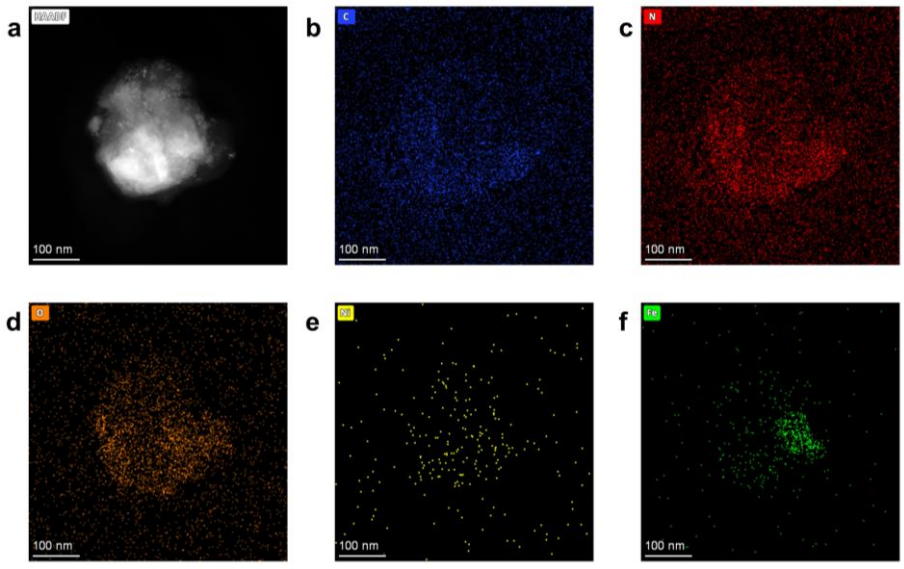

Fig. S11 (a) HAADF-STEM image and (b-f) the corresponding elemental mapping of C, N, O, Ni, and Fe for NFPB@CC after the CP test of 20 h.

To investigate the structural stability, NFPB@CC after the CP stability test of 20 h was

characterized by SEM in Fig. S10a. The particle density is not as good as before the test on account of the dissolution of NFPB at high electrode potentials. Nevertheless, there were still amounts of nano-cube NFPB particles that are firmly attached to the surface of the carbon fibers. As shown in Fig. S10b, the NFPB particle volume slightly decreased during the long period of oxidation test in comparison to pristine sample (Fig. S3d). It could be contributed to the oxidation and dissolved of species at the surface of NFPB particles under strong alkaline condition. From the low-resolution TEM image of Fig. S10c, it found that some uneven black spots attached to the surface of the particles which could be the products of NFPB transformation during the OER process. Furthermore, HR-TEM image of NFPB in Fig. S10d shows obvious single lattice with a crystal face spacing of 0.176 nm, corresponding to the (102) crystal face of $Ni(OH)_2$ (JCPDS NO. 14-0117). The HAADF-STEM image and the corresponding elemental mappings of NFPB demonstrate C, N, O, Ni, and Fe are uniformly distributed in Fig. S11. As shown in Fig. S11d, the content of O element increases significantly relative to that of the pristine sample which indicates that oxyhydroxide layer was formed in-situ electrochemically on the surface of NFPB.

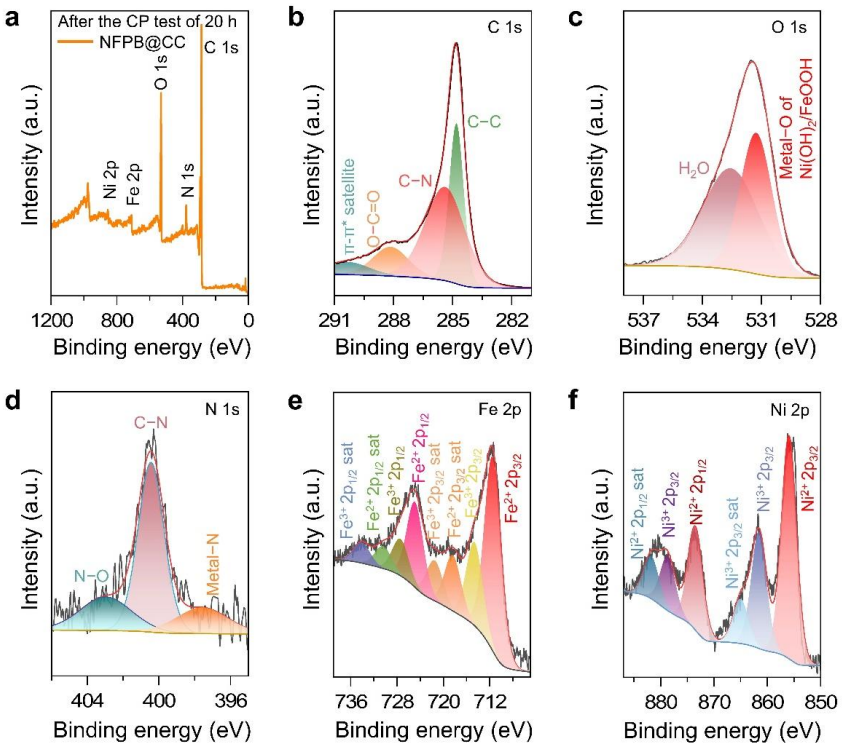

Fig. S12 (a) The XPS full spectrum of NFPB@CC after the CP test of 20 h. The XPS

spectra of (b) C 1s, (c) O 1s, (d) N 1s, (e) Fe 2p, and (e) Ni 2p for NFPB@CC.

To further verify the evolution process of NFPB composition during stability tests, the XPS spectrum of NFPB@CC was performed in Fig. S12. For the O 1s spectrum in Fig. S12c, the fitted peak of metal−O bond intensified by contrast with the pristine NFPB (Fig. 3c), which could be attributed to $Ni(OH)_2$ or (NiFe)OOH. As for the N 1s spectrum in Fig. S12d, the binding energy of N element become larger and positive shift than counterpart of the pristine NFPB (Fig. 3d). And the fitted peak at 403 eV is assigned to N−O bond, indicating the surface of NFPB particle was oxidized during CP test. Similarly, the binding energy of Fe element also show positive shift (Fig. S12e). It demonstrates that the electron cloud density around Fe decreases, which enhances the chemisorption of oxygen-containing intermediates and accelerates the OER process. It is worth mentioning that the peaks at 861.5 eV (Ni^{3+} $2p_{3/2}$) and 878.7 eV (Ni^{3+} $2p_{1/2}$) clearly distinguished from the Ni^{2+} $2p_{3/2}$ peak at 855.9 eV and Ni^{2+} $2p_{1/2}$ peak at 873.5 eV in Fig. S12f. It further demonstrates that the oxidation state of Ni species increased after OER as proved by the possible formation oxyhydroxide layer on the surface of NFPB@CC.[1]

Table S2

Comparison of OER activity of NFPB@CC with reported catalysts.

Sample	Electrolyte solution	Overpotential at 10 $mAcm^{-2}$	Tafel slope (mV/dec)	Reference
NFPB@CC	1 M KOH	332	78	This work
$NiCo_2O_4$/NiO	1 M KOH	380	50	Ref. S2
NiCoP/C	1 M KOH	330	96	Ref. S3
Fe_3O_4@Co_9S_8/rGO	1 M KOH	340	82.8	Ref. S4
$Co_{0.5}Fe_{0.5}S$@NMC	1 M KOH	410	159	Ref. S5

References

1 Z. Liu, Y. Wang, R. Chen, C. Chen, H. Yang, J. Ma, Y. Li and S. Wang, *J. Power Sources*, 2018, **403**, 90-96.

2 L. Han, X.-Y. Yu, X.-W.-D. Lou, *Adv. Mater.*, 2016, **28**, 4601-4605.

3 P. He, X.-Y. Yu, X.-W.-D. Lou, *Angew. Chem.*, 2017, **129**, 3955-3958.

4 J. Yang, G. Zhu, Y. Liu, J. Xia, Z. Ji, X. Shen, S. Wu, *Adv. Funct. Mater.*, 2016, **26**, 4712-4721.

5 M. Shen, C. Ruan, Y. Chen, C. Jiang, K. Ai, L. Lu, *ACS appl. Mater. & interfaces*, 2015, **7**, 1207-1218.

Movie S1 The water electrolysis process of NFPB@CC at 100 mA cm^{-2}.